Inorg. Chem. **2008**, *47*, 3452−3459

Coordination Chemistry of a π-Extended, Rigid and Redox-Active Tetrathiafulvalene-Fused Schiff-Base Ligand

Jin-Cai Wu,[†,‡] Shi-Xia Liu,[*,†] Tony D. Keene,[†] Antonia Neels,[§] Valeriu Mereacre,[⊥] Annie K. Powell,[⊥] and Silvio Decurtins[†]

Departement für Chemie und Biochemie, Universität Bern, Freiestrasse 3, CH-3012 Bern, Switzerland and Institut de Microtechnique, Université de Neuchâtel, Rue Jaquet Droz 1, CH-2002 Neuchâtel, Switzerland, and Institut für Anorganische Chemie, Universität Karlsruhe, Engesser Strasse 15, Geb. 30.45, D-76128 Karlsruhe, Germany

Received January 23, 2008

A π-extended, redox-active tetradentate tetrathiafulvalene-fused salphen [salphen = N,N′-phenylenebis(salicylideneimine)] compound (**L**) was prepared via a direct Schiff-base condensation of the corresponding diamine-tetrathiafulvalene (TTF) precursor with salicylaldehyde. Its chelating coordination ability has been demonstrated by the formation of the corresponding transition metal complexes in the presence of $M(OAc)_2 \cdot nH_2O$ (M = Co(II), Ni(II), Cu(II)) and $FeCl_3 \cdot 6H_2O$. Three complexes have been characterized by single-crystal X-ray diffraction analysis showing that the TTF-salphen ligand coordinates to the metal ions in a planar mode through the nitrogen and oxygen atoms in a N_2O_2 cis-configuration. In the case of Fe(III), a dinuclear oxo-bridged Fe(III) complex is formed. These paramagnetic complexes are promising building blocks for the construction of dual functional materials due to their unique structural features (planarity and rigidity) as well as their inherent redox properties.

Introduction

One of the current challenges in the field of materials chemistry is to prepare molecular conductors which are combined with additional spin carrier centers. Consequently, there have been many synthetic attempts for introducing paramagnetic metal ions into conducting molecular lattices which include, for instance, the redox-active tetrathiafulvalene (TTF) core.[1] A popular strategy to achieve an enhancement of π-d interactions in such dual-property materials is the direct coordination of paramagnetic metal ions to the potentially conducting organic assembly through intervening donor atoms from groups such as pyridine-type heterocycles,[2–4] and acetylacetonate ligands.[5] However, among the reported compounds revealing a direct coordination of paramagnetic metal ions to functionalized TTF

* To whom correspondence should be addressed. Tel.: 41 31 6314296. Fax: 41 31 6314399. E-mail: liu@iac.unibe.ch.
† Universität Bern.
‡ Present address: College of Chemistry and Chemical Engineering, Lanzhou University, 730000 Lanzhou, P. R. China.
§ Université de Neuchâtel.
⊥ Universität Karlsruhe.

(1) (a) Yamada, J-I. Sugimoto, T., Eds. *TTF Chemistry: Fundamentals and Applications of Tetrathiafulvalene*; Springer: Berlin, Germany, 2004. (b) Yamada, J-I.; Akutsu, H.; Nishikawa, H.; Kikuchi, K. *Chem. Rev.* **2004**, *104*, 5057. (c) Enoki, T.; Miyazaki, A. *Chem. Rev.* **2004**, *104*, 5449. (d) Coronado, E.; Day, P. *Chem. Rev.* **2004**, *104*, 5419. (e) Ouahab, L.; Enoki, T. *Eur. J. Inorg. Chem.* **2004**, 933. (f) Kobayashi, H.; Cui, H. B.; Kobayashi, A. *Chem. Rev.* **2004**, *104*, 5265.

(2) (a) Bouguessa, S.; Gouasmia, A. K.; Golhen, S.; Ouahab, L.; Fabre, J. M. *Tetrahedron Lett.* **2003**, *44*, 9275. (c) Liu, S-X.; Dolder, S.; Pilkington, M.; Decurtins, S. *J. Org. Chem.* **2002**, *67*, 3160. (d) Devic, T.; Avarvari, N.; Batail, P. *Chem. Eur. J.* **2004**, *10*, 3697. (e) Jia, C-Y.; Liu, S-X.; Tanner, C.; Leiggener, C.; Neels, A.; Sanguinet, L.; Levillain, E.; Leutwyler, S.; Hauser, A.; Decurtins, S. *Chem. Eur. J.* **2007**, *13*, 3804. (f) Jia, C-Y.; Liu, S-X.; Tanner, C.; Leiggener, C.; Sanguinet, L.; Levillain, E.; Leutwyler, S.; Hauser, A.; Decurtins, S. *Chem. Commun.* **2006**, 1878. (b) Liu, S-X.; Dolder, S.; Rusanov, E. B.; Stoeckli-Evans, H.; Decurtins, S. C. R. *C. R. Acad. Sci., Ser. IIc: Chim.* **2003**, *6*, 657.

(3) (a) Ota, A.; Ouahab, L.; Golhen, S.; Cador, O.; Yoshida, Y.; Saito, G. *New J. Chem.* **2005**, *29*, 1135. (b) Liu, S-X.; Dolder, S.; Franz, P.; Neels, A.; Stoeckli-Evans, H.; Decurtins, S. *Inorg. Chem.* **2003**, *42*, 4801. (c) Jia, C.; Liu, S-X.; Ambrus, C.; Neels, A.; Labat, G.; Decurtins, S. *Inorg. Chem.* **2006**, *45*, 3152. (d) Hervé, K.; Liu, S-X.; Cador, O.; Golhen, S.; Le Gal, Y.; Bousseksou, A.; Stoeckli-Evans, H.; Decurtins, S.; Ouahab, L. *Eur. J. Inorg. Chem.* **2006**, 3498. (e) Mosimann, M.; Liu, S-X.; Labat, G.; Neels, A.; Decurtins, S. *Inorg. Chim. Acta* **2007**, *360*, 3848. (f) Benbellat, N.; Gavrilenko, K. S.; Le Gal, Y.; Cador, O.; Golhen, S.; Gouasmia, A.; Fabre, J.-M.; Ouahab, L. *Inorg. Chem.* **2006**, *45*, 10440.

(4) (a) Setifi, F.; Ouahab, L.; Golhen, S.; Yoshida, Y.; Saito, G. *Inorg. Chem.* **2003**, *42*, 1791. (b) Liu, S-X.; Ambrus, C.; Dolder, S.; Neels, A.; Decurtins, S. *Inorg. Chem.* **2006**, *45*, 9622. (c) Lu, W.; Zhang, Y.; Dai, J.; Zhu, Q-Y.; Bian, G-Q.; Zhang, D-Q. *Eur. J. Inorg. Chem.* **2006**, 1629. (d) Avarvari, N.; Fourmigue, M. *Chem. Commun.* **2004**, 1300.

10.1021/ic800138x CCC: $40.75
Published on Web 03/28/2008

derivatives, the TTF moieties are mostly in the neutral state.[3] Up to now, only very few complexes with TTF ligands have been oxidized to afford their radical states.[4] However, they still show an insulating behavior due to dimerization[4a] and lack of highly ordered molecular stacking[4b,d] in the donor sublattice. In addition, it is noteworthy that a large variety of TTF derivatives which act as ligands toward metal ions have been studied in the fields of redox-active sensors, artificial antenna systems, and single-component molecular metals.[6]

Within this context, we focused our research on the synthesis of a planar π-extended TTF annulated N,N′-phenylenebis(salicylideneimine) (TTF-salphen) ligand, **L**, and its corresponding transition metal complexes. Analogous salen [salen = N,N′-ethylenebis(salicylideneimine)] complexes have been extensively studied as homogeneous catalysts for a variety of organic transformations[7] and as mimics of natural carriers in recognizing and transporting specific anions or neutral molecules.[8] Particular features of interest involve a transition metal's ability to effect catalytic reactions[9] or the binding capacity for small molecules (CO, O_2, NO, etc.).[10] Thereby, such studies might generate simple models for biologically occurring metalloproteins and metalloenzymes and help in a deeper understanding of biological systems.[11] It is suspected that the aforementioned biologically relevant chemical characteristics are directly related to the redox potential of the central metal ion in macrocyclic and Schiff-base complexes, which can be tuned by slight modifications of the imine bridges and substituents on the ligand framework.[12] As a consequence, much effort has been devoted to identify the factors that control the oxidation/reduction process in these complexes to determine their redox potentials and to characterize their electronic structures. Additionally, salen-type compounds are well-established in diverse research fields, for example, for liquid crystalline-[13] and nonlinear optical materials.[14]

Scheme 1. Molecular Structure of the TTF-salphen Ligand **L**

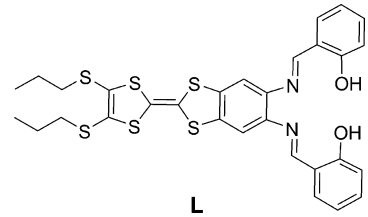

L

Following these considerations, a hitherto unknown π-extended TTF-salphen ligand **L** [salphen = N,N′-phenylenebis(salicylideneimine)], as shown in Scheme 1, has been prepared. Herein, we present the synthesis and molecular properties of **L** and extend our investigations to its coordinating ability toward various transition metal cations, such as Fe(III), Co(II), Ni(II), Cu(II).

Experimental Section

General. Unless otherwise stated, all reagents were purchased from commercial sources and used without additional purification. 5,6-diamino-2-(4,5-bis(propylthio)-1,3-dithio-2-ylidene)-benzo[*d*]-1,3-dithiole (**1**) was prepared according to literature procedures.[2e] Melting points were determined using a Büchi 510 instrument and

(5) (a) Massue, J.; Bellec, N.; Chopin, S.; Levillain, E.; Roisnel, T.; Clérac, R.; Lorcy, D. *Inorg. Chem.* **2005**, *44*, 8740. (b) Zhu, Q-Y.; Bian, G-Q.; Zhang, Y.; Dai, J.; Zhang, D-Q.; Lu, W. *Inorg. Chim. Acta* **2006**, *359*, 2303. (c) Pellon, P.; Gachot, G.; Le Bris, J.; Marchin, S.; Carlier, R.; Lorcy, D. *Inorg. Chem.* **2003**, *42*, 2056. (d) Bellec, N.; Massue, J.; Roisnel, T.; Lorcy, D. *Inorg. Chem. Commun.* **2007**, *10*, 1172.

(6) (a) Goze, C.; Leiggener, C.; Liu, S-X.; Sanguinet, L.; Levillain, E.; Hauser, A.; Decurtins, S. *ChemPhysChem* **2007**, *8*, 1504. (b) Dolder, S.; Liu, S-X.; Le Derf, F.; Sallé, M.; Neels, A.; Decurtins, S. *Org. Lett.* **2007**, *9*, 3753. (c) Zhao, Y.-P.; Wu, L.-Z.; Si, G.; Liu, Y.; Xue, H.; Zhang, L.-P.; Tung, C.-H. *J. Org. Chem.* **2007**, *72*, 3632. (d) Kobayashi, A.; Fujiwara, E.; Kobayashi, H. *Chem. Rev.* **2004**, *104*, 5243.

(7) (a) Zhang, F.; Bai, S.; Yap, G. P. A.; Tarwade, V.; Fox, J. M. *J. Am. Chem. Soc.* **2005**, *127*, 10590. (b) Larrow, J. F.; Jacobsen, E. N. *Top. Organomet. Chem.* **2004**, *6*, 123. (c) Che, C.-M.; Huang, J.-S. *Coord. Chem. Rev.* **2003**, *242*, 97. (d) Church, T. L.; Byrne, C. M.; Lobkovsky, E. B.; Coates, G. W. *J. Am. Chem. Soc.* **2007**, *129*, 8156. (e) Kleij, A. W.; Lutz, M.; Spek, A. L.; van Leeuwena, P. W. N. M.; Reek, J. N. H. *Chem. Commun.* **2005**, 3661. (f) Katsuka, T. *Adv. Synth. Catal.* **2002**, *344*, 131. (g) Kuil, M.; Goudriaan, P. E.; Kleij, A. W.; Tooke, D. M.; Spek, A. L.; van Leeuwena, P. W. N. M.; Reek, J. N. H. *Dalton Trans.* **2007**, 2311.

(8) (a) Yang, X. P.; Hahn, B. P.; Jones, R. A.; Wong, W.-K.; Stevenson, K. J. *Inorg. Chem.* **2007**, *46*, 7050. (b) Takao, K.; Ikeda, Y *Inorg. Chem.* **2007**, *46*, 1550. (c) Franceschi, F.; Guillemot, G.; Solari, E.; Floriani, C.; Re, N.; Birkedal, H.; Pattison, P. *Chem.—Eur. J.* **2001**, *7*, 1468. (d) Pecoraro, V. L.; Baldwin, M. J.; Gelasco, A. *Chem. Rev.* **1994**, *94*, 807. (e) Liu, Z. H.; Anson, F. C. *Inorg. Chem.* **2001**, *40*, 1329. (f) White, D. J.; Laing, N.; Miller, H.; Parsons, S.; Coles, S.; Tasker, P. A. *Chem. Commun.* **1999**, 2077. (g) Yamada, S. *Coord. Chem. Rev.* **1999**, *190−192*, 537. (h) Lu, X.-X.; Qin, S.-Y.; Zhou, Z.-Y.; Yam, V. W.-W. *Inorg. Chim. Acta* **2003**, *346*, 49. (i) van Doom, A. R.; Bas, M.; Harkema, S.; van Eerden, J.; Verboom, W.; Reinhoudt, D. N. *J. Org. Chem.* **1991**, *56*, 2371.

(9) (a) Leung, A. C. W.; MacLachlan, M. J. J. *Inorg. Organomet. Polym. Mater.* **2007**, *17*, 57. (b) Jing, H. W.; Edulji, S. K.; Gibbs, J. M.; Stern, C. L.; Zhou, H. Y.; Nguyen, S. T. *Inorg. Chem.* **2004**, *43*, 4315. (c) McMarrigle, E. M.; Gilheany, D. G. *Chem. Rev.* **2005**, *105*, 1563. (d) Escudero-Adán, E. C.; Benet-Buchholz, J.; Kleij, A. W. *Inorg. Chem.* **2007**, *46*, 7265. (e) Gallo, E.; Floriani, C.; Miyasaka, H.; Matsumoto, N. *Inorg. Chem.* **1996**, *35*, 5964. (f) Adam, W.; Fell, R. T.; Stegmann, V. R.; Saha-Möller, C. R. *J. Am. Chem. Soc.* **1998**, *120*, 708. (g) Li, Z.; Consar, K. R.; Jacobsen, E. N. *J. Am. Chem. Soc.* **1993**, *115*, 5326. (h) Horwitz, C. P.; Creager, S. E.; Murray, R. W. *Inorg. Chem.* **1990**, *29*, 1006.

(10) (a) Hoffman, B. M.; Szymanski, T.; Basolo, F. *J. Am. Chem. Soc.* **1975**, *97*, 637. (b) Zanello, P.; Cini, R.; Cinquantini, A.; Orioli, P. L. *J. Chem. Soc., Chem. Commun.* **1983**, 2159. (c) Chen, D.; Martell, A. E.; Sun, Y. *Inorg. Chem.* **1989**, *28*, 2647. (d) Cort, A. D.; Mandolini, L.; Pasquini, C.; Rissanen, K.; Russo, L.; Schiaffino, L. *New J. Chem.* **2007**, *31*, 1633.

(11) (a) Suslick, K. S.; Reinert, T. J. *J. Chem. Educ.* **1988**, *62*, 974. (b) Niederhoffer, E. C.; Timmons, J. H.; Martell, A. E. *Chem. Rev.* **1984**, *84*, 137. (c) Ueno, T.; Ohashi, M.; Kono, M.; Kondo, K.; Suzuki, A.; Yamane, T.; Watanabe, Y. *Inorg. Chem.* **2004**, *43*, 2852.

(12) (a) Freire, C.; de Castro, B. *J. Chem. Soc., Dalton Trans.* **1998**, 1491. (b) Thirumavalavan, M.; Akilan, P.; Kandaswam, M. *Polyhedron* **2005**, *24*, 1781. (c) Biswas, S.; Mitra, K.; Schwalbe, C. H.; Lucas, C. R.; Chattopadhyay, S. K.; Adhikary, B. *Inorg. Chim. Acta* **2005**, *358*, 2473. (d) Shimakoshi, H.; Takemoto, H.; Aritome, I.; Hisaeda, Y. *Tetrahedron Lett.* **2002**, *43*, 4809. (e) Kilic, A.; Tas, E.; Deveci, B.; Yilmaz, I. *Polyhedron* **2007**, *26*, 4009.

(13) (a) Abe, Y.; Nakabayashi, K.; Matsukawa, N.; Iida, M.; Tanese, T.; Sugibayashia, M.; Ohta, K. *Inorg. Chem. Commun.* **2004**, *7*, 580. (b) Paschke, R.; Balkow, D.; Sinn, E *Inorg. Chem.* **2002**, *41*, 1949. (c) Miyamura, K.; Mihara, A.; Fujii, T.; Gohshi, Y.; Ishii, Y. *J. Am. Chem. Soc.* **1995**, *117*, 2377. (d) Feringa, B. L.; van Delden, R. A.; Koumura, N.; Geertsema, E. M. *Chem. Rev.* **2000**, *100*, 1789.

(14) (a) Di Bella, S. *Chem. Soc. Rev.* **2001**, *30*, 355. (b) Delaire, J. A.; Nakatani, K. *Chem. Rev* **2000**, *100*, 1817. (c) Rigamonti, L.; Demartin, F.; Forni, A.; Righetto, S.; Pasini, A. *Inorg. Chem.* **2006**, *45*, 10976. (d) Powell, C. E.; Humphrey, M. G.; Cifuentes, M. P.; Morrall, J. P.; Samoc, M.; Luther-Davies, B. *J. Phys. Chem. A* **2003**, *107*, 11264. (e) Di Bella, S.; Fragalà, I.; Ledoux, I.; Diaz-Garcia, M. A.; Marks, T. J. *J. Am. Chem. Soc.* **1997**, *119*, 9550. (f) Tedim, J.; Patrício, S.; Bessada, R.; Morais, R.; Sousa, C.; Marques, M. B.; Freire, C. *Eur. J. Inorg. Chem.* **2006**, 3425.

Scheme 2. Synthetic Route to TTF-salphen Ligand **L**

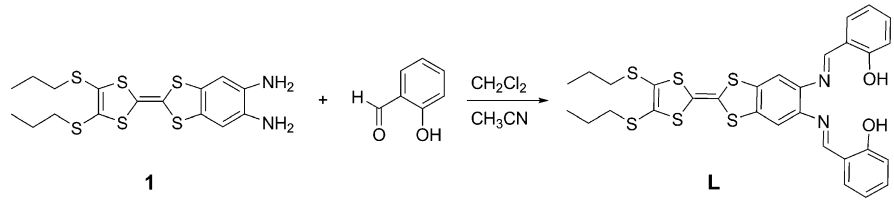

1 **L**

Table 1. Crystallographic Data

compd	**2**	**4**	**5**
formula	$C_{66}H_{66}Fe_2N_6O_7S_{12}$	$C_{33}H_{33}N_3NiO_3S_6$	$C_{32}H_{28}Cl_6CuN_2O_2S_6$
fw	1551.67	770.69	941.16
cryst. syst.	triclinic	monoclinic	monoclinic
space group	$P\bar{1}$	$P\ 2_1/c$	Cc
a (Å)	13.601(2)	16.3222(19)	39.121(6)
b (Å)	13.671(3)	18.031(3)	5.3371(5)
c (Å)	19.739(3)	11.8822(14)	20.584(3)
α (°)	83.321(14)	90	90
β (°)	71.904(12)	96.023(9)	118.426(11)
γ (°)	79.767(14)	90	90
V (Å^3)	3425.9(10)	3477.7(8)	3779.7(9)
Z	2	4	4
D_{calcd} (g cm^{-3})	1.504	1.472	1.654
μ (Mo Kα) (mm^{-1})	0.847	0.957	1.368
θ-range (deg)	1.52–25.20	1.69–25.05	1.18–25.15
indep. reflns	12205	6159	6050
obsd reflns [$I > 2\sigma(I)$]	2889	3264	3131
params refined	498	419	444
final R and R_w indices[a]	0.0710, 0.0906	0.0639, 0.1046	0.0930, 0.2248
largest diff. peak and hole (e Å^{-3})	0.368, –0.419	0.351, –0.720	0.819, –0.641

[a] $R = [\sum||F_o| - |F_c||)/\sum|F_o|]$; $R_w = [\sum(w(F_o^2 - F_c^2)^2)/\sum(wF_o^4)]^{1/2}$.

are uncorrected. Elemental analyses were performed on a Carlo Erba Instruments EA 1110 Elemental Analyzer CHN Carlo Erba Instruments. ^{1}H and ^{13}C NMR spectra were obtained on a Bruker AC 300 spectrometer operating at 300.18 and 75.5 MHz, respectively: chemical shifts are reported in ppm referenced to residual solvent protons ($CDCl_3$). The following abbreviations were used s (singlet), d (doublet), t (triplet), and m (multiplet). UV–vis absorption spectra were recorded on a Perkin-Elmer Lambda 10 spectrometer. Infrared spectra were recorded on a Perkin-Elmer Spectrum One FT-IR spectrometer using KBr pellets. EI spectra were recorded using an Auto SpecQ spectrometer. Cyclic voltammetry was conducted on a VA-Stand 663 electrochemical analyzer. An Ag/AgCl electrode containing 3 M KCl served as reference electrode, a glassy carbon electrode as counter electrode, and a Pt wire as working electrode. Cyclic voltammetric measurements were performed at room temperature under N_2 in CH_2Cl_2 with 0.1 M Bu_4NPF_6 as supporting electrolyte at a scan rate of 100 mV s^{-1}.

Synthesis of TTF-Salphen Ligand (L). A solution (2.16 g, 5 mml) of a 5,6-diamino-functionalized TTF derivative **1** (see Scheme 2) and salicylaldehyde (1.22 g, 10 mmol) in CH_2Cl_2/CH_3CN (1:3) was stirred overnight. The resulting precipitate was filtered, washed with ethanol, and then dried in a vacuum. The analytically pure ligand was obtained as an orange powder. Yield: 3.0 g (94%). Mp 173–175 °C, ^{1}H NMR ($CDCl_3$): δ = 1.03 (t, 6H), 1.67 (m, 4H), 2.82 (t, 4H), 6.92 (t, 2H), 7.04 (d, 2H, J = 9 Hz), 7.12 (s, 2H), 7.38 (m, 4H), 8.59 (s, 2H), 12.78 (s, 2H) ppm. ^{13}C NMR ($CDCl_3$): δ 13.16, 23.16, 38.32, 102.47, 112.60, 117.62, 119.07, 119.13, 127.87, 132.45, 133.69, 136.21, 141.05, 161.35, 163.52 ppm. IR (KBr): υ 3435, 2921, 1610 (vs), 1575, 1462, 1277, 1150, 1118, 913, 754 cm^{-1}. EIMS: m/z 640 [M]$^+$. Anal. Calcd (%) for $C_{30}H_{28}N_2O_6S_6$: C, 56.22; H, 4.40; N, 4.37. Found: C, 56.32; H, 4.40; N, 4.21. UV–vis (CH_2Cl_2): λ_{max} (lgε) 230 (4.65), 280 (4.65) 293 (4.67), 330 (4.70), 410 (4.20) nm.

Synthesis of [Fe(III)$_2$L$_2$(μ-O)] (2). To a solution of ligand **L** (64 mg, 0.1 mmol) and triethylamine (10 mmol) in CH_2Cl_2 was added an acetonitrile solution of $FeCl_3 \cdot 6H_2O$ (27 mg, 0.1mmol). The mixture was stirred at r.t. overnight. The resulting brown precipitate was filtered, washed with ethanol, and dried in a vacuum. The pure complex **2** was precipitated from a hot DMF solution as a deep orange powder. Yield: 50 mg (68%). Anal. Calcd (%) for $C_{60}H_{52}Fe_2N_4O_5S_{12} \cdot$DMF: C, 51.17; H, 4.02; N, 4.74. Found: C, 50.63; H, 4.17; N, 5.13. IR (KBr): υ 3436, 2921, 1604, 1530, 1453, 1367, 1254, 1228, 1191, 1149, 1124, 913, 814, 754, 579 cm^{-1}. UV–vis (CH_2Cl_2): λ_{max} (lgε) 230 (4.53), 305 (4.60), 328 (4.58), 397 (4.18), 480 (4.04) nm. X-ray-quality orange crystals were formed on cooling of a hot DMF solution of **2** after 1 day.

General Procedure for Preparation of Complexes 3–5. To a CH_2Cl_2 solution of ligand **L** (640 mg, 1 mmol) was added a CH_3CN solution of $M(OAc)_2 \cdot nH_2O$ (1.1 mmol), M = Co(II), Ni(II), Cu(II). After this mixture was stirred overnight, the resulting precipitate was collected, washed with ethanol, and dried in a vacuum. X-ray-quality single crystals of **4** and **5** were obtained by cooling of a DMF solution and a slow evaporation of a $CHCl_3$ solution, respectively.

[Co(II)L] (3). Yield: 89%. Anal. Calcd (%) for $C_{30}H_{26}CoN_2O_2S_6 \cdot H_2O$: C, 50.33; H, 3.94; N, 3.91. Found: C, 50.81; H, 3.71; N, 3.78. IR (KBr): υ 3435, 2922, 1605, 1524, 1451, 1362, 1331, 1266, 1236, 1149, 1122, 763, 752, 580 cm^{-1}. UV–vis (CH_2Cl_2): λ_{max} (lgε) 237 (4.67), 264 (4.74), 300 (4.64), 332 (4.70), 379 (4.37), 455 (4.40), 480 (4.40) nm.

[Ni(II)L] (4). Yield: 88%. Anal. Calcd (%) for $C_{30}H_{26}N_2NiO_2S_6$: C, 51.65; H, 3.76; N, 4.02. Found: C, 51.82; H, 3.73; N, 3.80. IR (KBr): υ 3436, 2921, 1605, 1524, 1451, 1362, 1329, 1264, 1234, 1196, 1149, 1122, 757, 580 cm^{-1}. UV–vis (CH_2Cl_2): λ_{max} (lgε) 238 (4.65), 264 (4.70), 300 (4.58), 331 (4.65), 379 (4.33), 455 (4.38), 480 (4.38) nm. ^{1}H NMR (DMSO-d_6): δ 0.97 (t, 6H), 1.56 (m, 4H),

Table 2. Selected Bond Lengths (Å) and Bond Angles (deg) of Compounds **2**, **4**, and **5**

2				**4**		**5**	
N(1)−Fe(1)	2.130(9)	C(11)−S(6)	1.761(13)	N(1)−Ni(1)	1.859(5)	N(1)−Cu(1)	1.970(12)
N(2)−Fe(1)	2.118(9)	C(11)−S(1)	1.771(13)	N(2)−Ni(1)	1.856(5)	N(2)−Cu(1)	1.946(13)
N(3)−Fe(2)	2.105(9)	C(12)−S(2)	1.744(12)	O(1)−Ni(1)	1.846(4)	O(1)−Cu(1)	1.875(10)
N(4)−Fe(2)	2.122(9)	C(12)−S(5)	1.760(12)	O(2)−Ni(1)	1.844(4)	O(2)−Cu(1)	1.885(10)
O(1)−Fe(2)	1.783(8)	C(41)−C(42)	1.330(14)	C(11)−S(4)	1.747(6)	C(11)−S(6)	1.713(16)
O(1)−Fe(1)	1.786(8)	C(41)−S(12)	1.750(12)	C(11)−S(1)	1.767(6)	C(11)−S(1)	1.749(16)
O(2)−Fe(1)	1.923(8)	C(41)−S(7)	1.769(13)	C(12)−S(3)	1.759(6)	C(12)−S(2)	1.73(2)
O(3)−Fe(1)	1.923(8)	C(42)−S(11)	1.741(12)	C(12)−S(2)	1.763(6)	C(12)−S(5)	1.746(17)
O(4)−Fe(2)	1.926(8)	C(42)−S(8)	1.768(12)	C(11)−C(12)	1.339(8)	C(11)−C(12)	1.41(2)
O(5)−Fe(2)	1.923(8)	C(11)−C(12)	1.353(14)				
Fe(2)−O(1)−Fe(1)	139.9(5)	O(2)−Ni(1)−O(1)	83.39(17)	O(1)−Cu(1)−O(2)	88.9(4)		
O(2)−Fe(1)−O(3)	92.7(3)	O(2)−Ni(1)−N(2)	94.92(19)	O(1)−Cu(1)−N(2)	176.6(5)		
O(3)−Fe(1)−N(2)	86.5(3)	O(1)−Ni(1)−N(2)	178.17(19)	O(2)−Cu(1)−N(2)	93.5(5)		
O(2)−Fe(1)−N(1)	86.2(3)	O(2)−Ni(1)−N(1)	177.23(17)	O(1)−Cu(1)−N(1)	91.7(5)		
N(2)−Fe(1)−N(1)	77.2(4)	O(1)−Ni(1)−N(1)	95.16(19)	O(2)−Cu(1)−N(1)	178.7(5)		
O(5)−Fe(2)−O(4)	90.9(4)	N(2)−Ni(1)−N(1)	86.6(2)	N(2)−Cu(1)−N(1)	85.9(5)		
O(4)−Fe(2)−N(3)	87.5(3)						
O(5)−Fe(2)−N(4)	86.8(3)						
N(3)−Fe(2)−N(4)	76.2(4)						

2.85 (t, 4H), 6.66 (t, 2H), 6.88 (d, 2H, $J = 9$ Hz), 7.32 (m, 2H), 7.50 (m, 2H), 8.31 (s, 2H), 8.88 (s, 2H).

[Cu(II)L] (5). Yield: 91%. Anal. Calcd (%) for $C_{30}H_{26}CuN_2O_2S_6$: C, 51.29; H, 3.73; N, 3.99. Found: C, 51.17; H, 3.69; N, 3.78. IR (KBr): υ 3435, 2921, 1607, 1523, 1451, 1368, 1328, 1260, 1228, 1186, 1148, 1122, 758, 575 cm^{-1}. UV–vis (CH_2Cl_2): λ_{max} (lgε) 241 (4.62), 265 (4.56), 328 (4.72), 440 (4.54), ~475 (4.44) nm.

Mössbauer Measurements. The Mössbauer spectra were acquired using a conventional spectrometer in the constant-acceleration mode equipped with a ^{57}Co source (3.7 GBq) in a rhodium matrix. Isomer shifts are given relative to α-Fe at room temperature. A constant sample temperature was maintained with an Oxford Instruments Mössbauer-Spectromag 4000 Cryostat. The spectra were fitted using NORMOS Mössbauer Fitting Program.

Magnetic Susceptibility. Magnetic susceptibility measurements were made on a Quantum Design MPMS SQUID-XL magnetometer in a field of 0.1 T between 300 and 1.86 K. Samples were prepared in gelatine capsules and held in plastic straws for mounting into the magnetometer. Diamagnetic corrections were made for the sample holder by measuring the empty gelatine capsule at room temperature and the correction for the sample was made using the approximation 0.4 × molecular weight × 10^{-6} cm^3 mol^{-1}.[15]

X-ray Crystallography. Crystals were mounted on a Stoe Mark II-Imaging Plate Diffractometer System (Stoe & Cie, 2002) equipped with a graphite-monochromator. Data collection was performed at –100 °C using Mo Kα radiation ($\lambda = 0.71073$ Å). In all cases, the resolution was $D_{max} - D_{min} = 24.00 - 0.82$ Å. The structures were solved by direct methods using the program SHELXS-97[16] and refined by full matrix least-squares on F^2 with SHELXL-97.[17] The hydrogen atoms were included in calculated positions and treated as riding atoms using SHELXL-97 default parameters. All non-hydrogen atoms were refined anisotropically. A semiempirical absorption correction was applied using DELrefABS (PLATON03,[18] $T_{min} = 0.311$, $T_{max} = 0.747$) and MULscanABS (PLATON03,[18] $T_{min} = 0.709$, $T_{max} = 0.863$) for **4** and **5**, respectively. The crystals of compound **4** were obtained as small thin needles resulting in a relatively weak diffraction of the analyzed crystal (parameter:observed reflections = 1:8). Nevertheless, the structure has been refined with acceptable standard uncertainties in bond lengths and angles. In the case of **2**, the crystal was only weakly diffracting (only about 25% of the data are observed, parameter:observed reflections = 1:6), which results in a low resolution structure with a reduced precision in bond distances and angles. Therefore, only the Fe, S, N and O atoms were refined anisotropically. A semiempirical absorption correction was applied using MULscanABS (PLATON03,[18] $T_{min} = 0.873$, $T_{max} = 0.893$). The crystallographic data are summarized in Table 1.

Results and Discussion

Synthesis and Characterization. TTF-salphen ligand (**L**) can be synthesized in 94% yield via the direct condensation reaction of salicylaldehyde with the diamine precursor **1**, as shown in Scheme 2. The ligand **L**, in its deprotonated dianionic form, provides a tetradentate N_2O_2 coordination sphere for metal ions. The corresponding transition metal complexes were obtained in good yields by combination of **L** with $M(OAc)_2 \cdot nH_2O$ (M = Co(II), Ni(II), Cu(II)) and $FeCl_3 \cdot 6H_2O$, respectively. All of them have been fully identified by elemental analysis, IR and NMR spectroscopy, mass spectra, electronic spectra and cyclic voltammetry, as well as magnetic susceptibility measurements (**2**) and X-ray single-crystal structure analyses (**2**, **4**, and **5**).

The IR spectrum of the ligand **L** shows a peak υ(C═N) at 1610 cm^{-1} as well as the phenol stretching vibration υ(C—O) at 1277 cm^{-1}. Upon complexation, these bands are shifted to lower frequencies indicating that the nitrogen atoms of the azomethine groups and oxygen atoms of the phenolate groups are coordinated to the metal ions. For the oxo-bridged diiron(III) complex **2**, the asymmetric stretching mode of the Fe—O—Fe unit occurs at 814 cm^{-1}, as expected.[19]

Due to the equivalent chemical environments, the ^{1}H NMR spectrum of the ligand **L** shows singlet peaks at 12.78 and 8.59 ppm, belonging to the OH and azomethine protons, respectively. Disappearance of the OH proton signal, as shown in ^{1}H NMR spectrum of **4**, indicates that **L** is deprotonated during complexation whereby the oxygen atoms take part in the coordination to Ni(II).

(15) Kahn, O. *Molecular Magnetism*; VCH Publishers: New York., 1993.
(16) Sheldrick, G. M. *Acta Crystallogr., Sect. A* **1990**, *46*, 467.
(17) Sheldrick, G. M. *SHELXL-97, Program for ®ment*; University of Göttingen: Göttingen, Germany, 1997.
(18) Spek, A. L. *J. Appl. Crystallogr.* **2003**, *36*, 7.
(19) (a) Ruan, W.-J.; Hu, G.-H.; Wang, S.-J.; Tian, J.-H.; Wang, Q.-L.; Zhu, Z.-A. *Chin. J. Chem.* **2005**, *23*, 709. (b) Kurtz, Jr; D, M. *Chem. Rev* **1990**, *90*, 585.

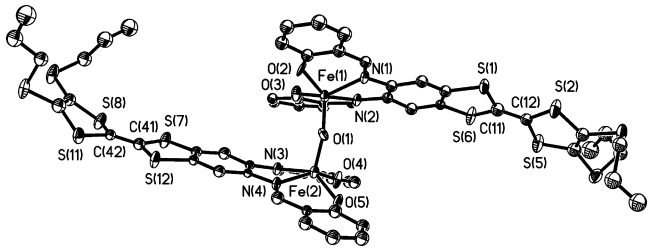

Figure 1. ORTEP diagram of **2** with thermal ellipsoids shown at the 50% probability level. Hydrogen atoms and solvent molecules are omitted for clarity.

The electronic absorption spectrum of ligand **L** in CH_2Cl_2 displays intense transitions in the range of 280–350 nm and a less intense broad absorption band in the visible, centered around 410 nm. The comparison with TTF[1a,2e,f,6a] and salen derivatives[14c,f,20] suggests that the former are comprised of several $\pi-\pi^*$ and $n-\pi^*$ transitions, essentially involving the TTF, azomethine and phenolate chromophore moieties present in the ligand. Specifically, the intense band at 330 nm is due to an intraligand charge-transfer from phenolate rings to the salphen moiety.[20c] The absorption in the visible region is attributed to an intramolecular $\pi-\pi^*$ charge-transfer transition from the TTF unit to the salphen fragment. Metalation of the free ligand leads to a red shift of charge-transfer transitions and to additional ligand to metal charge-transfer bands in the range of 350–400 nm (see Figure S1 in the Supporting Information).

Solid-State Structures of the Complexes 2, 4, and 5. The three solid state structures reveal, that the TTF-salphen ligand **L** acts, as expected, as a tetradentate ligand for metal ions with its two phenolate oxygens and two imine nitrogens as donor atoms. The relevant bond lengths and angles of the three compounds are listed in Table 2.

The neutral dinuclear complex [Fe(III)$_2$**L**$_2$(μ-O)] (**2**) crystallizes as the solvated compound **2**·2DMF in the centrosymmetric triclinic space group $P\bar{1}$. The asymmetric unit comprises the complete dinuclear entity, thus all atoms lie on general positions. A drawing of the compound is shown in Figure 1.

Two [Fe(III)**L**] complexes are linked by a bridging oxygen atom which occupies the apical position of the square pyramidal coordination geometry around each Fe(III) center. In their equatorial planes, the bond lengths Fe−N and Fe−O are quite similar to those of previously described Fe(III)-salphen complexes.[19,21] The Fe(1) and Fe(2) ions are displaced out of the least-squares planes defined by the N_2O_2 atoms by 0.552(5) and 0.575(5) Å, respectively. In comparison with other reported μ-oxo monobridged diiron complexes,[19,21] **2** has a similar average Fe−O(bridging) distance of 1.784 Å, but a relatively small Fe−O−Fe angle of 139.9(5)°. The annulated TTF backbones adopt a slightly boat-like conformation in both [Fe(III)**L**] units, which is quite typical for this heterocycle in its neutral state;[2a–f,22] the dihedral angles between the corresponding two five-membered rings (containing S1, S6 and S2, S5; S7, S12 and S8, S11) are 18.0(4) and 24.9(3)°, respectively. In the crystal packing (Figure 2), a segregation between the TTF and salphen units occurs along the *c*-axis and some close S···S contacts (S8···S9 = 3.523 Å; S2···S12 = 3.637 Å) are observed. However, there is no pronounced parallel head-to-head alignment of TTF units, as shown in the case of **5**, because of the steric constraints given by the specific dinuclear configuration. The complexes are linked along the *b*-axis via unconventional C–H···O (C···O = 3.200 Å; C–H···O = 151°) hydrogen bonds.

The neutral complex [Ni(II)**L**] (**4**) crystallizes as the solvated compound **4**·DMF in the centrosymmetric monoclinic space group $P2_1/c$ and the neutral complex [Cu(II)**L**] (**5**) as the solvated compound **5**·2$CHCl_3$ in the monoclinic space group *Cc*. In both cases, the asymmetric unit comprises the complete complex, thus all atoms lie on general positions. The drawings of the compounds are shown in Figures 3 and 4. The ligand **L** exhibits a pseudo-C_2 symmetry and coordinates the metal ions through the nitrogen and oxygen atoms in a planar N_2O_2 cis-configuration. Consequently, the coordination geometry around Ni(II) and Cu(II) is square planar and the metal ions are displaced out of the least-squares planes defined by the N_2O_2 atoms by 0.013(2) Å for Ni(II) and 0.010(6) Å for Cu(II). The central phenyl group of the TTF-salphen ligand makes the molecule rigid and planar, and as a consequence, the M−N bond distances are slightly longer than the M−O distances, a situation that is reversed in complexes with aliphatic bridges.[23] The N(1)···N(2) separations in **4** and **5** are 2.546 and 2.669 Å, respectively, whereas the bite angles N(1)−N−N(2) and N(1)−C−N(2) are 86.53 and 85.92°, respectively. The overall structural features compare well with those of known substituted [M(salen)] (M = Ni(II), Cu(II)) complexes.[23,24] In **4**, the TTF backbone adopts a boatlike conformation with a dihedral angle of 33.1(2)° between the two five-membered rings (containing S1, S4 and S2, S3), whereas in **5**, the TTF core is nearly planar with a dihedral angle of 6.3(9)° between the two five-membered rings (containing S1, S6 and S2, S5). Because of crystal packing effects, the propyl substituents in all compounds are arranged in a distinctly out-of-plane conformation.

In the crystal packing of **4** (Figure 5), the Ni(II) complexes are arranged nearly perpendicular to each other and some

(20) (a) Rotthaus, O.; Jarjayes, O.; Thomas, F.; Philouze, C.; Saint-Aman, E.; Pierre, J.-L. *Dalton Trans.* **2007**, 889. (b) Ilhan, S.; Temel, H.; Yilmaz, I.; ™ekerci, M. *Polyhedron* **2007**, *26*, 2795. (c) Khandar, A. A.; Shaabani, B.; Belaj, F.; Bakhtiari, A. *Inorg. Chim. Acta* **2007**, *360*, 3255. (d) Lever, A. B. P. *Inorganic Electronic Spectroscopy*, 2nd ed.; Elsevier: New York, 1984. (e) Bottcher, A.; Takeuchi, T.; Hardcastle, K. I.; Meade, T. J.; Gray, H. B.; Cwikel, D.; Kapon, M.; Dori, Z. *Inorg. Chem.* **1997**, *36*, 2498.

(21) (a) Davies, J. E.; Gatehouse, B. M *Acta Crystallogr., Sect. B* **1973**, *29*, 1934. (b) Oyaizu, K.; Dewi, E. L.; Tsuchida, E. *Inorg. Chim. Acta* **2001**, *321*, 205. (c) Mukherjee, R. N.; Stack, T. D. P.; Holm, R. H *J. Am. Chem. Soc.* **1988**, *110*, 1850.

(22) Wu, J.-C.; Liu, S.-X.; Neels, A.; Le Derf, F.; Sallé, M.; Decurtins, S. *Tetrahedron* **2007**, *63*, 11282.

(23) (a) Manfredotti, A. G.; Guastini, C. *Acta Crystallogr,. Sect. C* **1983**, *39*, 863. (b) Radha, A.; Seshasayee, M.; Ramalingam, K.; Aravamudan, G. *Acta Crystallogr., Sect. C* **1985**, *41*, 1169. (c) Akhtar, F. *Acta Crystallogr., Sect. B* **1981**, *37*, 84.

(24) (a) Bhadbhade, M. M.; Srinivas, D. *Inorg. Chem.* **1993**, *32*, 5458. (b) Marzilli, L. G.; Summers, M. F.; Bresciani, N.; Pahor, E.; Charland, J.-P.; Randaccio, L. *J. Am. Chem. Soc.* **1985**, *107*, 6680. (c) Cassoux, C.; Gleizes, A. *Inorg. Chem.* **1980**, *19*, 665. (d) Zhang, S.-S.; Yang, B.; Wang, Y.-F.; Li, X.-M.; Jiao, K. *Asian J. Chem.* **2005**, *17*, 929.

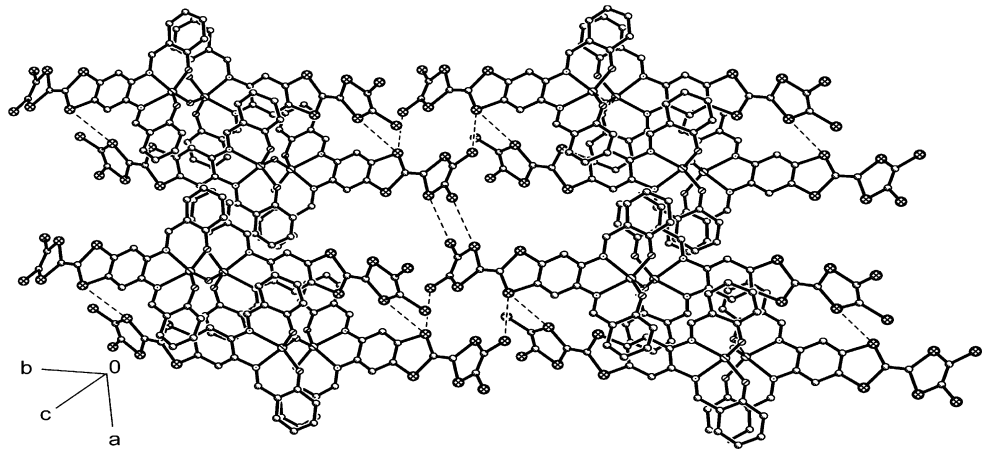

Figure 2. Packing diagram of **2**. The S···S contacts are depicted as dashed lines; hydrogen atoms and solvent molecules as well as propyl groups are omitted for clarity.

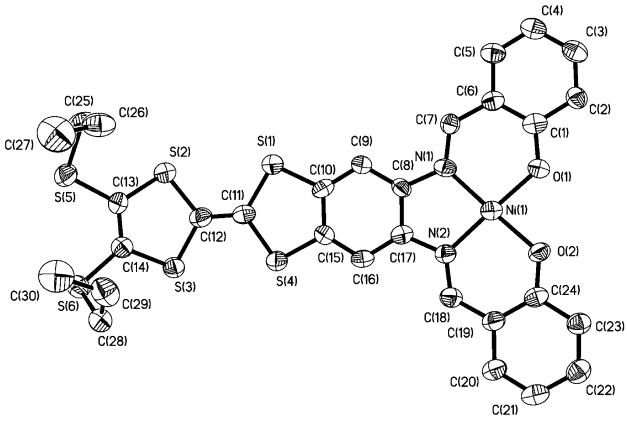

Figure 3. ORTEP diagram of **4** with thermal ellipsoids shown at the 50% probability level. Hydrogen atoms and solvent molecules are omitted for clarity.

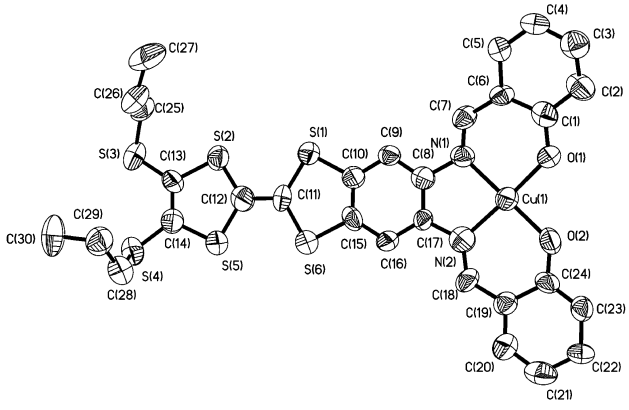

Figure 4. ORTEP diagram of **5** with thermal ellipsoids shown at the 50% probability level. Hydrogen atoms and solvent molecules are omitted for clarity.

unconventional C–H···O (C···O 3.362–3.430 Å; C–H···O 147–152°) hydrogen bonds and S···Ni (3.813 Å) close contacts are observed. In addition, the molecules are stacked in pairs via $\pi\cdots\pi$ interactions with a distance of 3.282 Å between the mean planes through the salphen moieties. Figure 6 highlights the mutual arrangement of the Cu(II) complexes in the crystal structure of **5**. A noticeable feature is the parallel head-to-head alignment with intermolecular S···S contacts of 3.651 Å. In the crystal lattice, the molecules exhibit some unconventional C–H···Cl (C···Cl = 3.56 Å; C–H···Cl = 142°), C–H···S (C···S = 3.119 Å; C–H···S = 109°) and C–H···O (C···O = 3.09–3.14 Å; C–H···O = 132–154°) hydrogen bonds.

Electrochemical Properties. The electrochemical properties of compounds **L** and **2**−**5** were investigated by cyclic voltammetry in CH_2Cl_2 (Table 3). In each compound, the TTF-salphen ligand undergoes two well-separated (quasi)reversible one-electron oxidation processes to the radical cation and dication states, corresponding to $E_{1/2}(1)$ and $E_{1/2}(2)$, respectively. Upon coordination, the observed redox potentials for the TTF oxidation processes remain almost unchanged and the peak-to-peak separations ($\Delta E_p = E_{pa} - E_{pc}$) are similar to or somewhat larger than those observed for the free ligand. It can therefore be deduced that the presence of the metal ions in the salphen cavity seems to have a negligible influence on the redox potentials of the TTF moiety. This behavior can be ascribed to the complexation induced deprotonation, which keeps the overall charges balanced. The larger ΔE_p in most of the present complexes indicates that diffusion-controlled (quasi)reversible redox processes are expected to occur under the experimental conditions used, as shown in Figure S2 of the Supporting Information. Moreover, ΔE_p increases at high scan rates indicating the quasi-reversible nature of the electron transfer processes for the oxidation of the TTF unit and the reduction of metal ions. Complexes **2**, **3** (Figures S3 and S4 in the Supporting Information) and **5** show a reversible Fe(III/II), Co(II/I), and Cu(II/I) redox process, respectively. In the case of **3**, at a high scan rate, the irreversible oxidation process Co(II) → Co(III) + e^- occurs at 0.15 V in the first cycle while a cathodic peak (E_{pc}) appears at –0.67 V, corresponding to the irreversible reduction of the resulting Co(III) species upon scanning through a second cycle.

Mössbauer Spectra. ^{57}Fe Mössbauer spectroscopy has been applied to provide a direct probe of the electronic structure and chemical environments of the two iron(III) sites in complex **2**.[19b] Zero-field Mössbauer spectra of **2** at 77

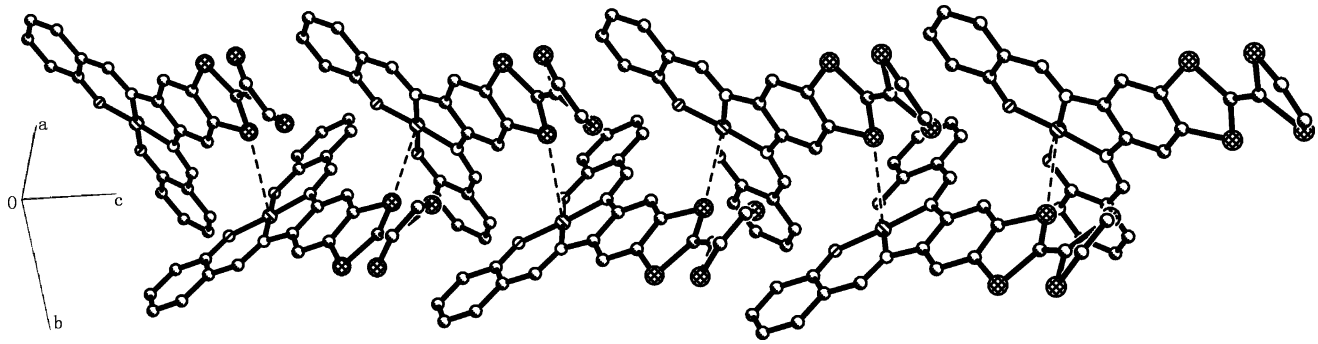

Figure 5. Packing diagram of **4**. The S···Ni close contacts are depicted as dashed lines; hydrogen atoms and solvent molecules as well as propyl groups are omitted for clarity.

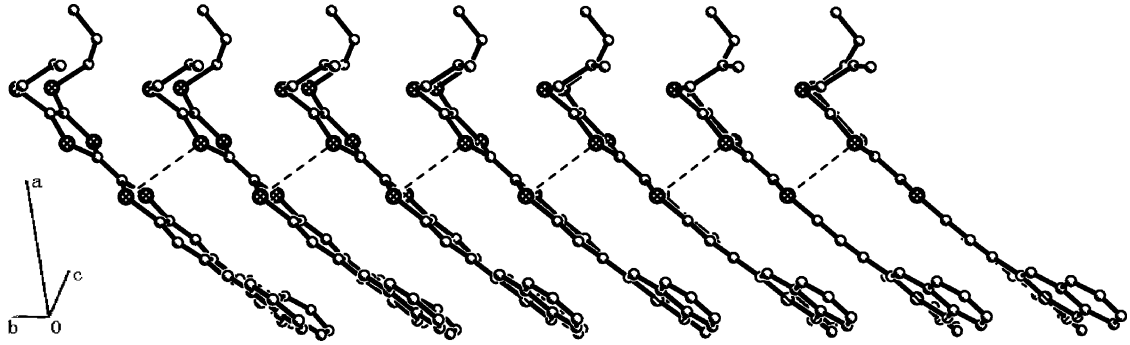

Figure 6. Packing diagram of **5**. The S···S close contacts are depicted as dashed lines; hydrogen atoms and solvent molecules are omitted for clarity.

Table 3. Cyclic Voltammetric Data

	oxidation (*E*/V)						reduction (*E*/V)	
compd	$E_{pc}(1)$	$E_{pa}(1)$	$E_{1/2}(1)$	$E_{pc}(2)$	$E_{pa}(2)$	$E_{1/2}(2)$	$E_{1/2}^{M(III/II)}$	$E_{1/2}^{M(II/I)}$
L	0.56	0.64	0.60	0.94	1.03	0.98		
2	0.58	0.65	0.61	0.98	1.06	1.05	−0.33[a]	
3	0.48	0.65	0.57	0.92	1.07	1.00	−0.67[b]	−1.42[a]
4	0.51	0.75	0.63	0.85	1.18	1.01		
5	0.58	0.65	0.62	0.94	1.06	1.00		−1.16

[a] At a 1 V/s scan rate. [b] Additional anodic peak appears at 0.15 at a 1 V/sscan rate.

and 3 K are shown in Figure 7. They consist of sharp, symmetrical quadrupole doublets. Every spectrum could also be fit with two overlapping doublets assigned to two positions with only weak deviations indicating the presence of the two crystallographically independent iron sites in **2**. The isomer shifts (IS) and quadrupole splitting (QS) values (IS = 0.43, QS = 0.72 mm s^{-1} and IS = 0.42, QS = 0.71 mm s^{-1}) at 3 and 77 K, respectively, are typical parameters for high-spin Fe(III) (S = 5/2) centers.[19b,25] These results are in good agreement with the single crystal structure analysis (charge balance) and the magnetic investigation.

Magnetic Properties. The magnetic susceptibility of **2** (Figure 8) shows a χ_M value of 4.07 × 10^{-3} cm^3 mol^{-1} at 300 K, which decreases almost imperceptibly with decreasing temperature, until it increases rapidly below 40 K to a value of 45.0 × 10^{-3} cm^3mol^{-1} at 1.86 K. A plot of $\chi_M T$(T) (Figure

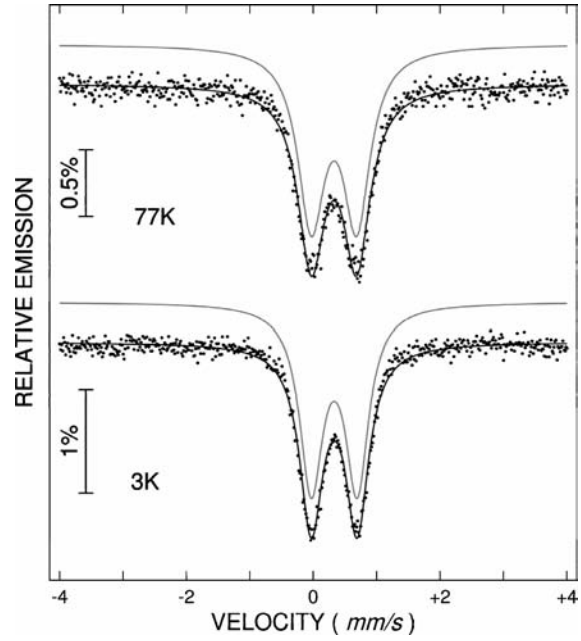

Figure 7. ^{57}Fe Mössbauer spectra for **2** at 77 and 3 K.

8) shows a decreasing product on cooling with a small feature below ~60 K where the gradient decreases before dropping away again below ~40 K. A Curie–Weiss fit was not attempted with the inverse susceptibility plot as the spins appear to be distinctly coupled at room temperature. Given the molecular structure of **2** and the decreasing value of $\chi_M T$ on cooling, it is most likely the dominant interaction is that of an antiferromagnetic dimer.

The $\chi_M T$ data was modeled using an S = 5/2 dimer model derived from the isotropic exchange Hamiltonian $H = -2JS_AS_B$

(25) (a) Nichols, P. J.; Fallon, G. D.; Murray, K. S.; West, B. O. *Inorg. Chem.* **1988**, *27*, 2795. (b) Kennedy, B. J.; Brain, G.; Horn, E.; Murray, K. S.; Snow, M. R. *Inorg. Chem.* **1985**, *24*, 1647. (c) Kennedy, B. J.; McGrath, A. C.; Murray, K. S.; Skelton, B. W.; White, A. H. *Inorg. Chem.* **1987**, *26*, 483. (d) Berry, K. J.; Clark, P. E.; Murray, K. S.; Ralston, C. L.; White, A. H. *Inorg. Chem.* **1983**, *22*, 3928. (e) Renz, F.; Hill, D.; Klein, M.; Hefner, J. *Polyhedron* **2007**, *26*, 2325.

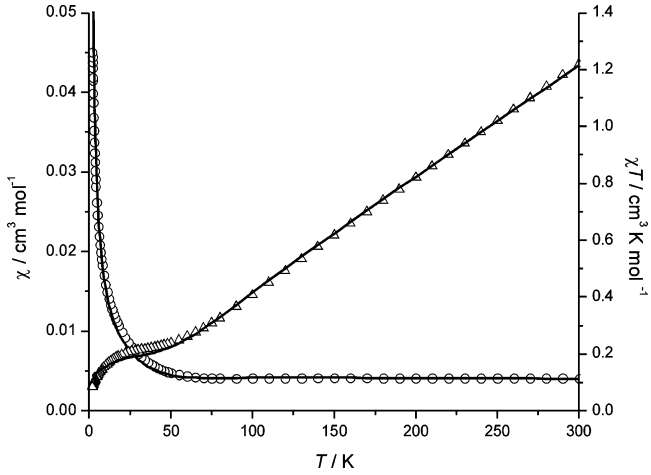

Figure 8. Plot of $\chi_M(T)$ (circles) and $\chi_M T(T)$ (triangles), both with fit to eq 1, for compound **2**.

with an additional term to account for a monomeric $S = 5/2$ impurity with zero-field splitting (1)

$$\chi_M = (1-p)\left[\frac{2Ng^2\mu_B^2}{k_B T}\frac{e^x + 5e^{3x} + 14e^{6x} + 30e^{10x} + 55e^{15x}}{1 + 3e^x + 5e^{3x} + 7e^{6x} + 9e^{10x} + 11e^{15x}}\right] + p(\alpha) \quad (1)$$

where $x = 2J/k_B T$, α is a term for a zero-field split Fe(III) monomeric impurity[15] and p is the ratio of the impurity.

From this fit, we obtain $g = 1.98(5)$, $2J = -84(1)$ cm^{-1} and $p = 0.049(1)$. The values of g and $2J$ fit well within the ranges reported for oxo-bridged Fe(III) dimers.[19,26]

(26) (a) Ercolani, C.; Gardini, M.; Murray, K. S.; Pennesi, G.; Rossi, G. *Inorg. Chem.* **1986**, *25*, 3972. (b) Ercolani, E.; Gardini, M.; Monacelli, F.; Pennesi, G.; Rossi, G. *Inorg. Chem.* **1983**, *22*, 2584.

Conclusions

The syntheses, molecular structures, optical and redox behavior of a TTF-fused salphen ligand and its corresponding transition metal complexes are described. As expected, the redox-active π-extended tetradentate ligand coordinates to the metal ions through nitrogen and oxygen atoms in a N_2O_2 cis-configuration. The coordination geometry around Ni(II) and Cu(II) is essentially square planar, whereas in the case of **2**, both [Fe(III)(TTF-salphen)] units are linked by one bridging oxygen atom which occupies the apical position of a square pyramidal coordination geometry around each Fe(III) ion. Studies of the magnetic susceptibilities of the oxo-bridged Fe(III) complex reveal an intramolecular antiferromagnetic coupling similar to that of analogous oxo-bridged Fe(III) compounds. The Mössbauer spectra confirms the $S = 5/2$ spin values for the Fe(III) centers. The molecular structures of these complexes, especially the rigidity and planarity together with their redox properties, render them promising for the elaboration of hybrid organic–inorganic materials. Consequently, the studies on chemical and electrochemical partial oxidation of these compounds may pave the way to obtain multifunctional materials and these projects are currently under investigation in our laboratory.

Acknowledgment. This work was supported by the Swiss National Science Foundation (Grant 200020–116003 and COST Action D31).

Supporting Information Available: CIF files for **2**, **4**, and **5**; the absorption spectra and cyclic voltammograms of the ligand **L** and complexes **2**−**5** (PDF). This material is available free of charge via the Internet at http://pubs.acs.org.

IC800138X